IRAQI Academic Scientific Journals

Tikrit Journal of Engineering Sciences (2020) 27 (2): 71-81

ISSN: 1813-162X (Print) ; 2312-7589 (Online)

Tikrit Journal of Engineering Sciences

available online at: http://www.tj-es.com

TJES Tikrit Journal of Engineering Sciences

College of Engineering

Gaeid KS, Uddin MN, Mohamed MK, Mohmmoud ON. Design and Implement of Dual Axis Solar Tracker System Based Arduino. *Tikrit Journal of Engineering Sciences* 2020; **27**(2): 71- 81.

Khalaf S Gaeid[1*]

M Nasir Uddin[2]

Mohamed K Mohamed [1]

Omar N Mohmmoud[1]

[1] Electrical Department/ Engineering College/Tikrit University /Tikrit, Iraq

[2] Department of Electrical Engineering/Lakehead University/Canada

K e y w o r d s

Photovoltaic (PV), Solar Tracker, Sensor Light-Dependent Resistor (LDR), LM35, Relay, Satellite motor.

A R T I C L E I N F O

Article history:

Received 07 Dec. 2019

Accepted 10 May 2020

Available online 01 July 2020

Design and Implement of Dual Axis Solar Tracker System Based Arduino

A B S T R A C T

The computer control plays important role in the solar cell design and development of dual axis solar tracker for the sun's position. The main goal of this paper is to maximize energy output to reduce panel temperature (cooling), to increase efficiency of the PV panel. Small-scale solar is developed through a complete hardware and software in order to function accurately. The main parts in this work are Arduino Uno R3, kit relay, LDR (Light Dependent Resistor), LM35 (temperature sensor), high-efficiency solar panel and satellite motor. The Protuse software is used with (Arduino Uno) as embedded computer control. The results show the effectiveness of the complete tracking system.

DOI: http://doi.org/10.25130/tjes.27.2.09

السيطرة الحاسوبية على منظومة تتبع شمسي ثنائية المحور

خلف سلوم كعيد / قسم الهندسة الكهربائية /كلية الهندسة/جامعة تكريت/العراق، محمد نصير الدين / قسم الهندسة الكهربائية / كلية الهندسة/ جامعة ليكهيد/كندا
محمد كريم محمد /قسم الهندسة الكهربائية /كلية الهندسة/جامعة تكريت/العراق، عمر نافع محمود /قسم الهندسة الكهربائية /كلية الهندسة/جامعة تكريت/العراق

الخلاصة

ان الغرض الرئيسي من هذا العمل هو تقديم فكرة تقوم على تصميم وتطوير منظومة تعقب الطاقة الشمسية التلقائي لتحقيق أقصى قدر من انتاج الطاقة وأيضا للحد من درجه حرارة اللوحة ، لزيادة الكفاءة الكهروضوئية قام الفريق في هذه البحث، بتطوير نظام التتبع الشمسي التلقائي لنظام الطاقة الشمسية الصغيرة النطاق. وقد تم تطوير جزء الأجهزة وجزء البرمجة في وقت واحد من أجل نظام تتبع الطاقة الشمسية للحصول على منظومة تعمل بدقة عالية. تم استعمال اردوينو اونو، المقاومة الضوئية (LDR)، حساس درجه الحرارة(LM35)، لوحه عالية الكفاءة للطاقة الشمسية، المحركات الخاصة بالسيطرة على الصحن المستخدم لالتقاط إشارة بث القنوات الفضائية، برنامج Protuse لمحاكاة لغة البرمجة عالية المستوي وقد تم تضمينها في الأجهزة لتشغيل نظام التتبع والتبريد بشكل فعال. وقد اظهر نظام التتبع والتبريد فعالية كبيرة في توصيل الطاقة إلى ألواح الطاقة الشمسية.**الكلمات الدالة:** البوليمرات الحيوية، الدمك، احتمالية الانهيار، التربة الجبسية، مقاومة القص، صمغ الزنثان.

1. INTRODUCTION

In the last decade, many of the residential around the world used the electric solar system as a sub power at their houses. This is because solar energy is an unlimited energy resource, set to become increasingly important in the longer term, for providing electricity and heat energy

* *Corresponding author: E-mail:* gaeidkhalaf@gmail.com

to the user. Solar energy also has the potential to be the major energy supply in the future [1].

The energy of the sun is the prime source and it is considered as the fuel for most of the renewable systems. The photovoltaic (PV) system is used to replace the sun energy resources [2]. Electrical energy comes directly from conversion of the solar energy through the inverters and solar panel. These panels are constructed from silicon and germanium semiconductor materials with low efficiency [3]. To increase the performance, the intensity of light falling on the solar panel should be increased. Solar trackers are considered the most suitable technology to enhance the efficiency. The enhancement is carried out through keeping the solar panels tracking the sun's position. Recently, the trackers are the much common way to increase the efficiency in spite of the increasing cost [4].

In the past, people using solar energy fix the panels' mid-way between the geographical east and west with approximately 30 degrees towards the south [5].

Studies have shown that this is not the ideal positioning in order to maximize energy extraction. A better way is to orient the panels continuously towards the sun, using single or double axes. Many researchers have published papers on the subject [6]. For a fossil fuel, efficient microcontroller based sun tracker control for solar cell systems is introduced in [7].

Ghazanfar Mehdia et al. (2019) designed a sun tracker where the sun position is sensed using photo transistors connected to frame and mounted on a simple structure [8]. The internet of things (IoT), is one of the future control approach in the smart buildings and industry with interconnected micro grids.

Dual axis system was designed, implemented and the performance evaluated using light dependent resistor (LDR) sensors, direct current (DC) motors [9]-[10]. One of the dual axes solar tracking is shown in Fig.1.

The proposed technique in this work is based on simple and easily programmed Arduino as a Microcontroller (MC) of the dual axis automatic solar tracker to ensures effectiveness and feasibility of the design methodology.

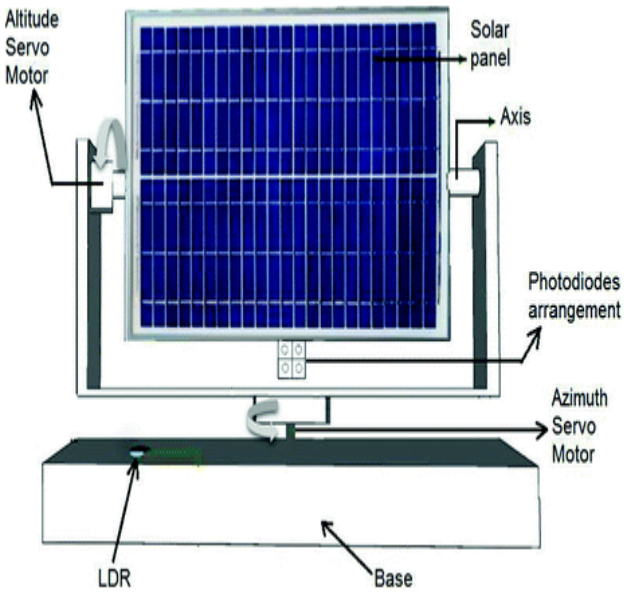

Fig.1. Dual axis solar tracking [11]

The temperature sensor is used to reduce panel temperature (cooling) by a water pumping motor.

The block diagram of a dual-Axis tracking system is shown in Fig.2.

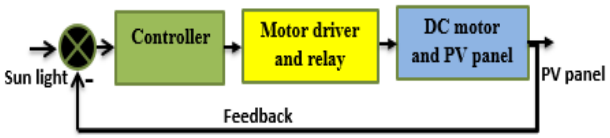

Fig.2. Block diagram of a Dual-Axis Tracking System [12]

The contributions of this work are: perfect tracking and cooling system and studying the behavior of the PV panel. The first case deals with tracker, the second case is the cooling function, and the third case is the tracking and cooling function with static behavior but without cooling.

2. MATERIALS AND METHODS

The main parts of the proposed techniques are illustrated as a block diagram shown in Fig.3. These parts includecollective, sensor, a microcontroller and motor units. The sensor unit is composed of LDR Light Dependent Resistor and LM35 temperature sensor [13]. The LDR functions in the presence and absence of light. The LDR function is to detect the sunlight in order to obtain the direction of the solar irradiation maximum power. The LDR movement tracking will increase the concentration of the energy by the solar that assists to realize its function efficiently.

The LM35 is a temperature sensor that checks temperature degree and decide to run the motor pump or not.

The Uno [14] controls the LDR and LM35 signals as a micro controller in the closed loop solar tracking system. One of the advantages of Arduino is the open-source code on reading input and output ports [15]. Few calculations are required for the input signals using different formulas for the signals received. The microcontroller (MC) sends a signal to both of the satellite motor and water pump.

The overall transfer function of the motor used with U(s) as the control input signal is expressed in (1) [16];

$$\frac{\theta_0(s)}{U(s)} = \frac{k}{(js+f)(L_a s+R_a)+k^2} * \frac{1}{s(js+f)} \quad (1)$$

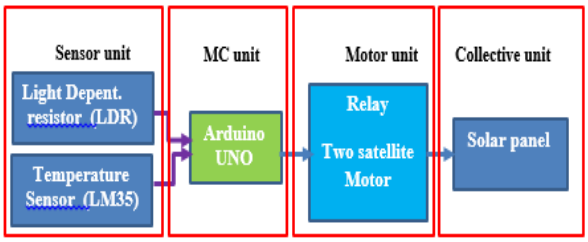

Fig. 3. The automatic solar tracker main parts

The dual axis tracker algorithm used is shown in Fig. 4. The steps of the flowchart start with supplying the controller with power supply followed by LDR measurement for the light intensity difference for all four LDRs. The motor rotates in vertical or clockwise direction when LDR1signal is greater than LDR2 signal. The same manner is used for horizontal motor. In addition, turn on pump motor when temperature degree is greater than 25 C°.

The state-space model of the solar tracking system for the PV panels driven by DC motors is given in [17].

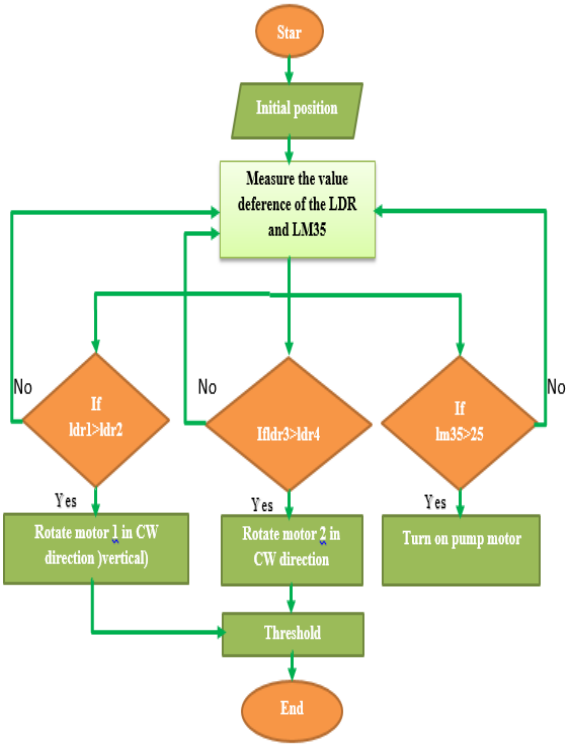

Fig 4. The system flow chart

$$\frac{d}{dt}\begin{bmatrix}\theta\\ \theta^{\cdot}\\ i\end{bmatrix} = \begin{bmatrix}0 & 1 & 0\\ 0 & -b/L & k/J\\ 0 & -K/L & -R/J\end{bmatrix}\begin{bmatrix}\theta\\ \theta^{\cdot}\\ i\end{bmatrix} + \begin{bmatrix}0\\ 0\\ 1/L\end{bmatrix}V$$

$$y = [1\ \ 0\ \ 0]\begin{bmatrix}\theta\\ \theta^{\cdot}\\ i\end{bmatrix}$$

(2)

$$A = \begin{bmatrix}0 & 1.0000 & 0\\ 0 & -0.0012 & 0.4763\\ 0 & -9.5904 & -33.8983\end{bmatrix},\quad B = \begin{bmatrix}0\\ 0\\ 341.2969\end{bmatrix},$$

$$C = [1\ \ 0\ \ 0]$$

Where

$\theta, \theta^{\cdot}, i$ is the position of the DC motor, speed and current respectively

The transfer function of the DC motor obtained from the state space representation is shown in (3)

$$TF = \frac{162.5}{s^3 + 33.9\,s^2 + 4.609\,s + 2.754e-15} \quad (3)$$

3. EXPERIMENTAL WORK

The hardware implementation consists of control circuit that contains multiple combinations of electronic components the hardware implementation is divided into 2 parts:

1. The detection part
2. The movement part.

The LDR sensor is used to detect the light intensity and lm35 sensor to detect temperature degree. The movement section consists of two satellite motors to rotate the dual axis. Reverse direction for every motor attempt by reverse polarity so will use relay to reverse polarity.

In many cases, the system presents a nonlinear phenomenon which is fully characterized by its static characteristics, i.e., its dynamics can be neglected [18]. The ideal relay behavior is shown in Fig.5.

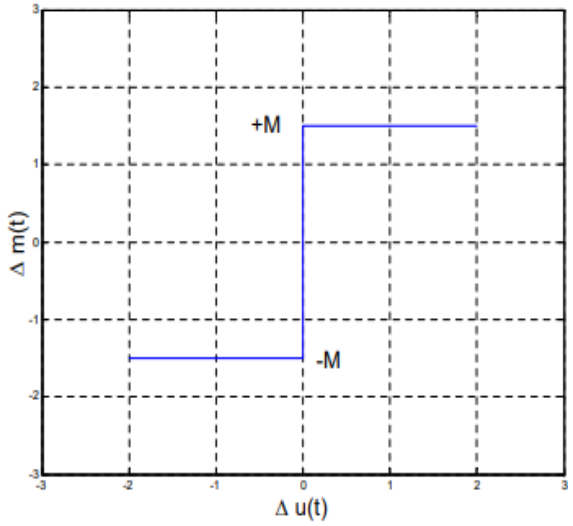

Fig.5.The behavior of nonlinear relay

The describing function (DF) approach to the analysis of steady-state oscillation in nonlinear systems is an approximate tool to estimate the limit cycle parameters. It is based on the assumptions of one single nonlinear component and the nonlinear component is not dynamical and time invariant [19]. The Fourier transform is used to analyze the DF of the system [20] as in (4)

$$y(t) = \frac{a_o}{2} + \sum_{k=1}^{\infty} (a_k \sin(k\frac{2\pi}{T}t) + b_k \cos(k\frac{2\pi}{T}t)) \quad (4)$$

The coefficients (a_k and b_k) of the Fourier response is given in (5) and (6) respectively , a_o is the DC level in the output response.

$$a_k = \frac{2}{T} + \int_{-T/2}^{T/2} f(t)\cos(k\frac{2\pi}{T}t)dt = \frac{1}{\pi}\int_{-\pi/2}^{\pi/2} f(t)\cos(k\frac{2\pi}{T}t)d(\frac{2\pi}{T}t) \quad (5)$$

$$b_k = \frac{2}{T} + \int_{-T/2}^{T/2} f(t)\sin(k\frac{2\pi}{T}t)dt = \frac{1}{\pi}\int_{-\pi/2}^{\pi/2} f(t)\sin(k\frac{2\pi}{T}t)d(\frac{2\pi}{T}t) \quad (6)$$

Where bo=0 for the k=0, 1, 2, 3,…..

$$a_k = \frac{2}{T}\int_{-T/2}^{T/2} \Delta m(t)\cos(\omega t)dt = 0 \quad (7)$$

Because it's odd symmetry of the Δm (t)

$$b_k = \frac{2}{T}\int_{-T/2}^{T/2} \Delta m(t)\sin(\omega t)dt = \frac{4}{\pi}\int_{0}^{\pi/2} M\sin(\vartheta)d\vartheta = \frac{4M}{\pi} \quad (8)$$

Hence, the proposed model function can be calculated as a describing function of the fundamental component of the output to the amplitude of the given input.

$$Describing\ \ function(DF) = \frac{4M}{U\pi} = \frac{20}{U\pi} \quad (9)$$

Each of the above is critical for the project's hardware implementation. As mentioned earlier, the Arduino Uno R3; relay kit connects satellite motors to Arduino Uno

R3, LDR as sensors, LM35 sensor, high efficiency solar panels with 3.31A, 54W are used to complete the setup.

3.1 Detection part

The combination of 4LDR sensors formed the sensing part with Arduino Uno R3.The implementation of the proposed algorithm is shown in the schematic diagram in Fig. 6.

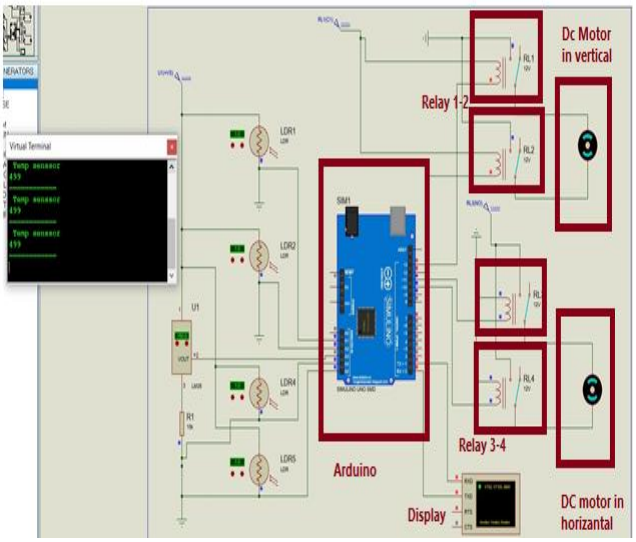

Fig. 6. Automatic Solar Tracker Hardware

The fabrication of the detection part will be according to the interconnection of the four LDRs and LM35 with Arduino Uno R3. As shown in the schematic diagram in Fig. 7, each sensor is connected to the analog port (A1, A2, A3, A4 and A5) to give analog inputs to the MC. The programming code for the four LDRs and LM35 is compiled into the Arduino Uno R3.

The signals tested through an observation conducted by using the Arduino IDE software. In Fig.7, part of software program that shows the difference in light intensity and temperature degree.

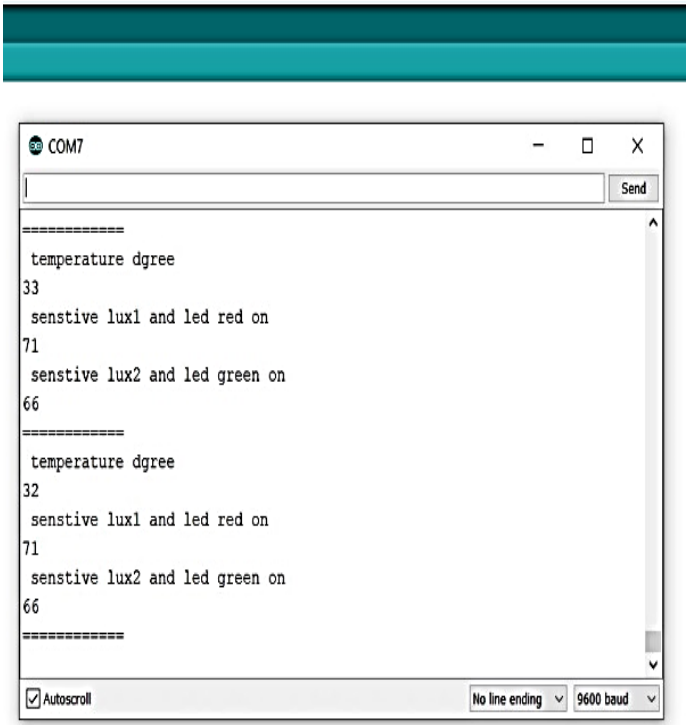

Fig.7. Sensors values

Now testing sensors during a sunny day is shown in Table 1. The resistance of an LDR may typically have the following resistances: Daylight = 5000Ω and dark = 20000000Ω

Table 1. Temperature degree and light intensity (Lux) between two LDR in horizontal axis.

Hours	LDR1(C^0)	LDR2(C^0)	LM35(C^0)
8	60	54	22
9	70	65	25
10	70	67	25
11	71	66	30
12	76	70	35
13	75	69	34
14	77	70	35
15	65	59	34
16	59	52	25
17	40	39	19

The line graph of intensity (Lx) converted to Celsius for two LDR from 8 to 17 hours is shown in Fig.8.

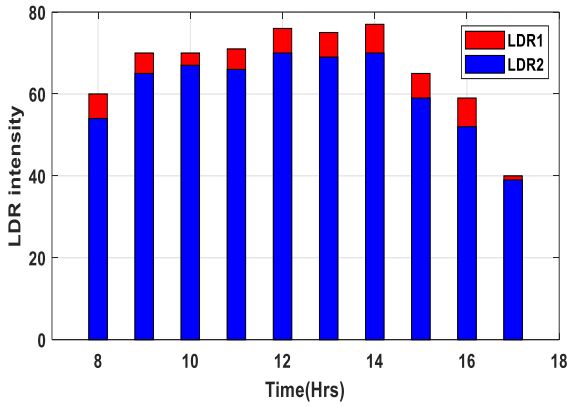

Fig. 8. LDR intensity versus Time for horizontal axis during sunny day.

3.2 Motion Part

The motion part is composed of Arduino Uno R3 and two motors. The interconnections of the part are shown in the schematic diagram of Fig. 6. In this Figure, four relays are used for forward and reverse direction of motor for controlling it in both axis.

A kit of four relays (SRD-05 VDC) is used as gates to pass the suitable voltage to the motors. First two relays are used to power on the motor in clockwise direction. Whereas the third and fourth relays are used to power the same motor in the reverse direction (counter clockwise), as shown in Fig.9.

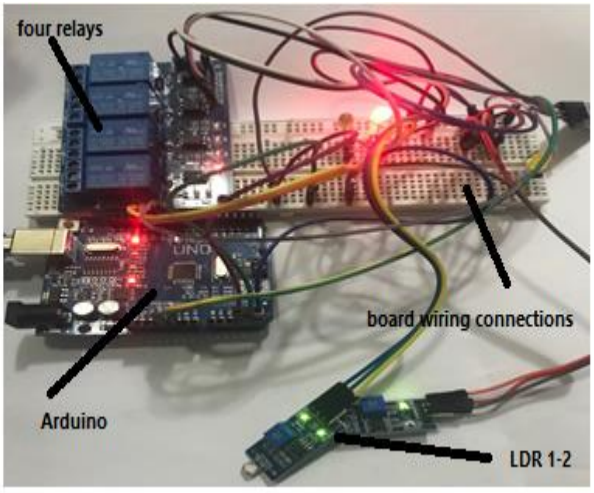

Fig.9. Control circuit

Considering the linear relationship between light intensity and the produced voltage, the microcontroller can produce the resolution in angle (θ_R) as in (10) [21].

$$\theta_R = \cos^{-1}(V_{oc} - 0.5V_R / V_{oc}) \quad (10)$$

Where,

V_{OC}, V_R, δ, α is the open-circuit voltage reference voltage, open-circuit voltage of the PV panel, angle between the backs of the panels and horizontal plane and the angle of the sun to some reference point respectively [22].

The angle between the normal to the faces of the panels as in (11).

$$\beta = 180 - \delta \quad (11)$$

The voltage across PV panel as in (12).

$$V_{pv} = 0.5V_{oc}[\cos((\alpha - \theta_i) \pm \beta/2) + 1] \quad (12)$$

The above relationships according to the sunlight compared to the horizontal plane and place of the PV panel is shown in Fig.10 [23]-[24].

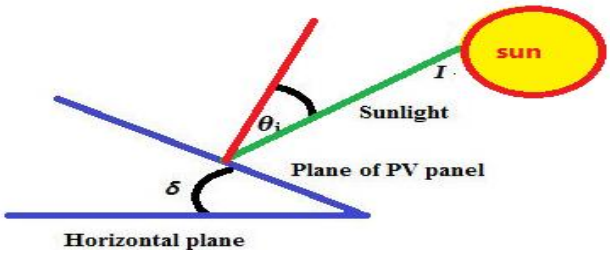

Fig.10. PV panel and sunlight position relationship in the dual axis tracking

The panel surfaces is heated due light radiation so it needs cooling to increase the efficiency and live time. The panel cooling is performed with air to reduce the cost [25].

1. RESULTS AND DISCUSSION

The measurements with and without tracking system to obtain the clear view of the features of using solar based solar PV tracking system. The monitoring of these features is recorded for two days with same loads and periods .In the first day (22nd November 2019), the PV response output response is monitored without using the

tracking system. In the second day (23th November, 2019) the PV output response has been measured using timer based tracking system. It is noticed that the LDR based tracking system enhance the output power of PV panel systems. The differentiation between LDR based PV tracking system with non-tracking system is shown in the Tables 2, 3, 4 and Table 5. The PV output response increased with tracking system and decreased without tracking system. In all cases, the load is connected to the system.

The data in Tables 2, 3, 4 and Table 5 show that the automatic solar tracker produces more power compared to the static solar panel as shown in (Fig.14 and Fig.18), the proposed system has the higher average power than static solar panel.

Table 2. Response system measurements under load in 1st day (3.31A, 54W)

Hours	Voltage (V)	Current(A)	Power(W)
8	18.2	0.84	15.288
9	19.05	1.66	31.623
10	20.5	2.12	43.46
11	20.65	2.99	61.7435
12	20.66	3.1	64.046
13	20.56	3.19	65.5864
14	20	3.1	62
15	20.1	2.89	58.089
16	19	1.5	28.5
17	10	0.67	6.7

The standard deviation and the average power of Table 2 are shown in Fig.11.

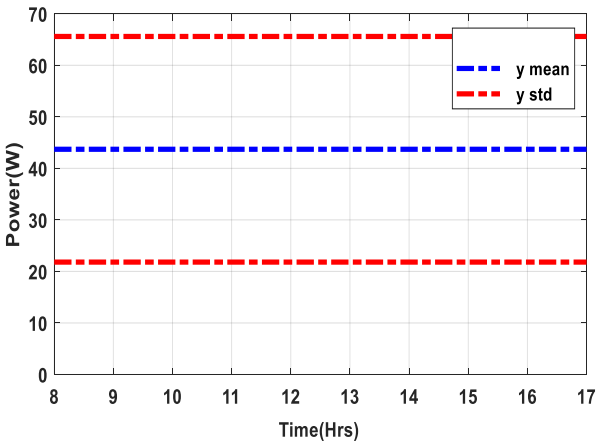

Fig.11. Standard deviation and mean power

In the standard deviation (y_{std}) figure, the square of the variance is the basis for knowing the quality of estimation procedures for the mean (y_{mean}) as important parameters.

The percentage of each power day of Table 2 out of the total power is shown in Fig.12.

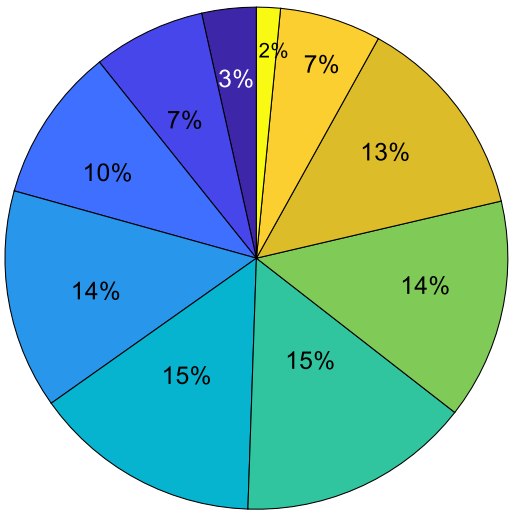

Fig.12. Pie chart of daily output power as in Table 2

Table 3. Response system measurements under load in 1st day (3.31 A, 54 W)

Hours	Voltage(V)	Current(A)	Power(W)
8	21.7	2.03	44.051
9	19.5	2.55	49.725
10	20.57	2.98	61.298
11	20.77	3.09	64.179
12	20.86	3.2	66.752
13	21	3.22	67.62
14	21.1	3.3	69.63
15	20.2	3.1	62.62
16	19.3	2.9	55.97
17	10.25	2	20.5

The standard deviation and the average power of Table 3 is shown in Fig.13.

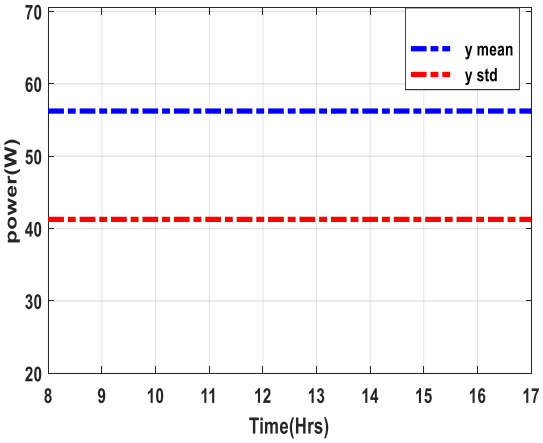

Fig.13. Standard deviation and mean power

The power readings collected from (8 to 17) hours for first day is shown in Fig.14.

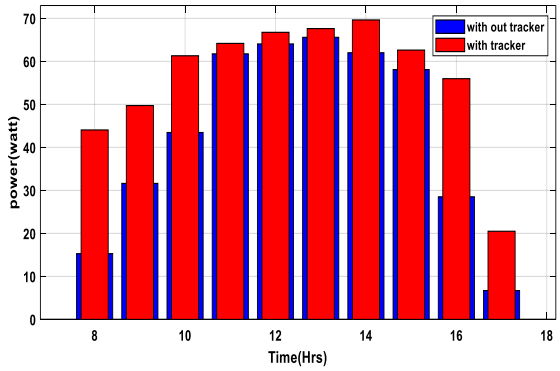

Fig.14. The power without tracker and with tracker for 1st day.

The percentage of each power day of Table 3 out of the total power is shown in Fig.15. The amounts of powers are increasing (up from 4 percent in the morning and 12 percent in midday to 8 percent in the last hour of the experiment).

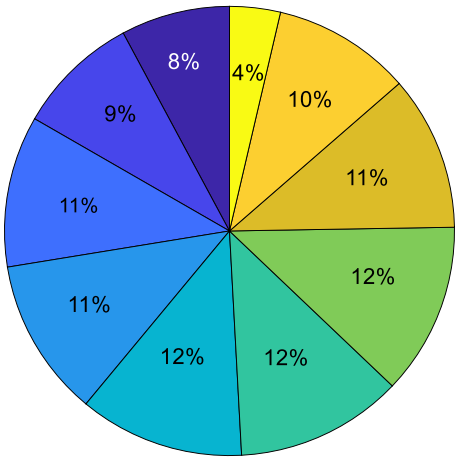

Fig.15. Pie chart of daily output power of Table 3

Table 4. Response system measurements under load in the 2nd day (3.31A, 54W)

Hours	Voltage(V)	Current(A)	Power (W)
8	18.02	0.8	14.416
9	18.9	1.55	29.295
10	20.2	2.1	42.42
11	20.43	2.65	54.139
12	20.5	2.95	60.475
13	20.55	3.12	64.116
14	20.23	3.15	63.724
15	20.2	2.8	56.56
16	18.98	1.4	26.572
17	12	0.69	8.28

The standard deviation and the mean power of Table 4 are shown in Fig.16.

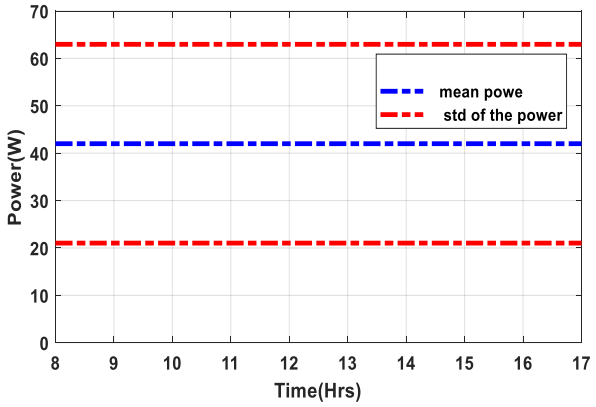

Fig.16.The standard deviation and the average power during the operation hours

The percentage of each daily power can be illustrated as in Fig.17.

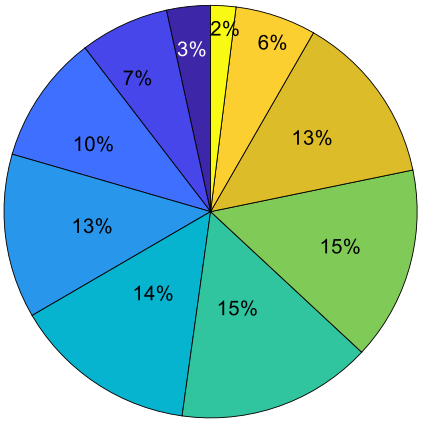

Fig.17. Pie chart of daily output power percentage

Table 5. Response system measurements under load in 2nd day (3.31 A , 54 W)

Hours	Voltage(V)	Current(A)	Power(W)
8	21.43	1.63	34.931
9	19.32	2.65	51.198
10	20.44	3.00	61.32
11	20.57	3.08	63.355
12	20.81	3.13	65.135
13	20.88	3.14	65.563
14	20.94	3.23	67.636
15	19.8	3.05	60.39
16	19.2	2.35	45.12
17	13.2	1.25	16.5

The power measurements collected from 8 hours to 17 hours for second day is shown in Fig 18.

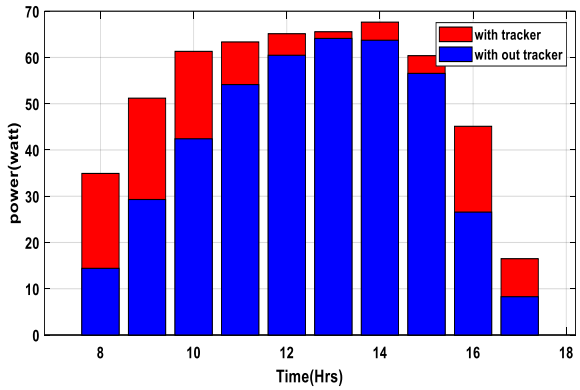

Fig.18. The power without tracker and with tracker for the 2nd day

The output energy comparison in terms of power with tracker and without sun tracker for two days is represented in this graph of Fig.14 and Fig.18. It is noticed that, the output energy with sun tracker PV Panel systems has higher value.

The standard deviation and the average value of the power can be shown in Fig.19.

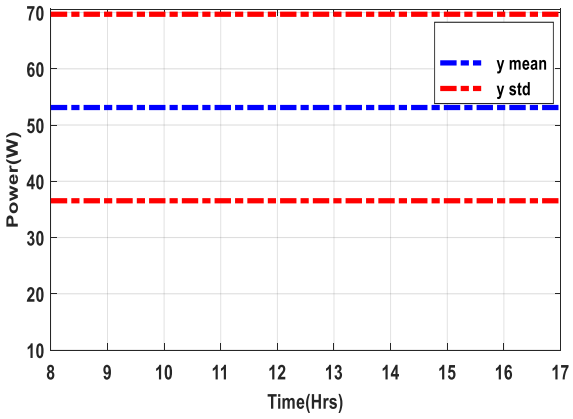

Fig.19. Standard deviation and the mean of the power

Testing the controllability and observability shows, the system is completely controllable and observable as in the matrices below

$$ctrb = 1.0e+05 * \begin{bmatrix} 0 & 0 & 0.0016 \\ 0 & 0.0016 & -0.0551 \\ 0.0034 & -0.1157 & 3.9062 \end{bmatrix}$$

(13)

$$obsv = \begin{bmatrix} 1.0000 & 0 & 0 \\ 0 & 1.0000 & 0 \\ 0 & -0.0012 & 0.4763 \end{bmatrix}$$

(14)

The rank of both of the above two matrices is a full rank matrix. The Bode plot of the complete system with nonlinear element effect (blue) and the system without the nonlinear element (relay) (red) effect is shown in Fig.20.

This effect is reduced with low pass filter in the feedback to compensate the nonlinearity behavior.

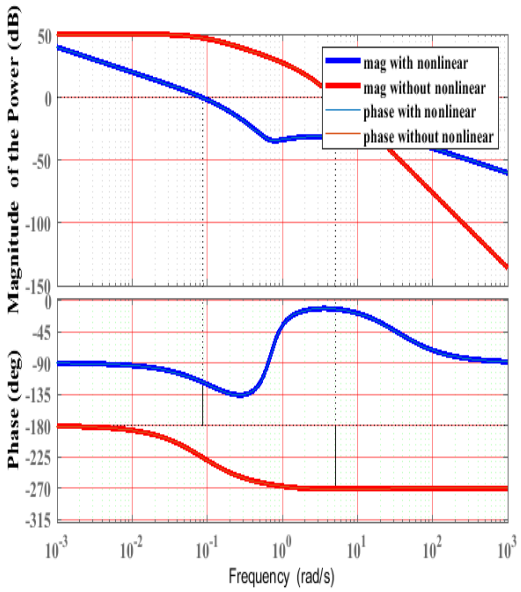

Fig.20.Bode plot of the complete system with and outshout the nonlinear element

In nonlinear systems, when the input sinusoidal is applied to the system, the nonlinear element is a function of frequency and input amplitude as in Fig. 21. Describing function shows that the nonlinearity reduced with the increase of input amplitude, which satisfy the nonlinearity, is time-invariant.

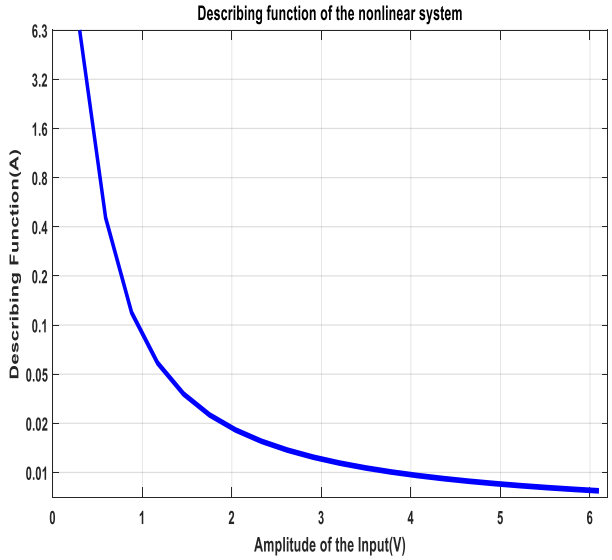

Fig.21.DF of the complete system with the nonlinear element

5. CONCLUSIONS

In this paper, the dual axis tracker computer control is presented to obtain maximum power from the solar energy over the conventional static solar panel and without cooling. The system is fabricated and investigated successfully. The proposed technique has an advantage because it uses satellite motor as an actuator device to produce a much higher performance and less power consumption compared to the stepper motor. This system is cost effective, simple, efficient and it operates automatically.

REFERENCES

[1] Ayush Goel, Tarun Prakash. Sun Tracking Solar Panel. Project in Jaypee University of Information and Technology. Himachal Pradesh; 2019.

[2] H. K Ringkjob, P. M. Haugan, Astrid Nybo. Transitioning Remote Arctic Settlements to Renewable Energy Systems–A Modelling Study of Longyearbyen, Svalbard. Applied Energy, 2020; 258:114079.

[3] H.K. Ringkjob, P.M. Haugan, I.M. Solbrekke. A Review of Modelling Tools for Energy and Electricity Systems with Large Shares of Variable Renewables. Renew Sustain Energy Rev, 2018; 96, 440-459.

[4] Jamilu Ya'u Muhammad, Mohammed Tajudeen Jimoh, brahim Baba Kyari, Mohammed Abdullahi Gele, Ibrahim Musa. A Review on Solar Tracking System: A Technique of Solar Power Output Enhancement. Engineering Science, 2019; 4(1): 1-11.

[5] Jim Skea, Renée van Diemen, Matthew Hannon, Evangelos Gazis, Aidan Rhodes. Energy Innovation for the Twenty-First Century. Edward Elgar Publishing, 2019.

[6] Zakaria El Jaouhari, Youssef Zaz, Salah Moughyt, Omar El Kadmiri, Zakaria El Kadmiri. Dual-Axis Solar Tracker Design Based on a Digital Hemispherical Imager. J. Sol. Energy Eng, 2019; 141(1):1-8.

[7] Mod H. Arif, J. Hossen, G. Ramana Murthy, Jesmeen M. Z. H., J. Emerson Raja. An Efficient Microcontroller Based Sun Tracker Control for Solar Cell Systems. International Journal of Electrical and Computer Engineering, 2019; 9(4):2742-2750.

[8] Ghazanfar Mehdia. Design and Fabrication of Automatic Single Axis Solar Tracker for Solar panel. 2nd International Conference on Computing, Mathematics and Engineering Technologies (iCoMET), Sukkur, Pakistan, 2019.

[9] Soumya Das Suprava, Chakraborty Suprava, Chakraborty Pradip, Kumar Sadhu, Pradip Kumar, Sadhu O. S. Sastry, O. S. Sastry. Design and Experimental Execution of a Microcontroller (µ C)-Based Smart Dual-Axis Automatic Solar Tracking System. Energy Science and Engineering, 2015; 3(6):558–564.

[10] Murdan A.P., Jugurnauth R., Nirsimloo R.R. .Design and Implementation of a Smart Dual Axis Solar Tracker with an Anti-theft Alarm Mechanism. In: Fleming P., Vyas N., Sanei S., Deb K. (eds) Emerging Trends in Electrical, Electronic and Communications Engineering.

ELECOM 2016. Lecture Notes in Electrical Engineering, vol. 416. Springer, Cham, 2017.
[11] Hachimenum Nyebuchi .Design and Performance Evaluation of a Dual - Axis Solar Tracking System for Rural Applications. European Journal of Electrical and Computer Engineering, 2019; 3(1):1-6.
[12] Echendu, R.E., Amadi, H.N. Design and Implementation of an Off-Grid Solar Tracker Control System using Proteus Version 8.1. IOSR Journal of Engineering (IOSRJEN), 2018; 8(4): 4-12.
[13] Shoroug Alweheshi, Aisha Abdelali, Muhanad Albarassi, Ahmed Hammoda, Adel Mohamed. Simulation and Hardware Implementation of Photovoltaic Maximum Power Point Tracking System. International Conference on Power Generation Systems and Renewable Energy Technologies, Turkey, 2019.
[14] Harish, S.V, Suhas, S., Abhina, V, Harish, S, Vinayaka, R. Solar Panel Maintenance System. IJISE, 2019; 1(2): 1-10.
[15] Joysankha Ghosh, Pabak Das. Automatic Solar Tracking System. Degree of Bachelor of Technology in Applied Electronics & Instrumentation Engineering, RCC Institute of Information Technology,India,2019.
[16] Mbaocha C. C, Eze C. U, Ezenugu I. A, Onwumere J. C. Satellite Model for Yaw-Axis Determination and Control Using PID Compensator. International Journal of Scientific & Engineering Research, 2016; 7(7), 1623-1629.
[17] Quang Ha, Manh Duong Phung. IoT-Enabled Dependable Control for Solar Energy Harvesting in Smart Buildings. IET Research Journal, 2019; 3:1-12.
[18] Elio Usai. Describing Function analysis Describing Function Analysis of Nonlinear Systems. University of Cagliari lectures, 2015; 1-84.
[19] D.Prsica,C.Fragassa, N.Nedica, A.Pavlovic. Describing Function of the Pneumatic Flapper-Nozzle Valve. Mechanical Systems and Signal Processing, 2019; 124:696-714.
[20] Rahoma AU,Hassan AH. Fourier Transforms Investigation of Global Solar Radiation at True Noon: in the Desert climatology. American Journal of Applied Sciences, 2007; 4(11): 902-907.
[21] Issarachai Ngamroo. Wide-Area Damping Controllers of Wind and Solar Power Using Probabilistic Signal Selection. IET Renewable Power Generation, 2019; 13(8):1351 – 1359.
[22] Mousazadeh, H., Keyhani, A., Javadi, A., Mobli, H., Abrinia, K., Sharifi, A. A Review of Principle and Sun-Tracking Methods for Maximizing Solar Systems Output. Renew. Sustain. Energy Rev, 2009; 13(8):1800–1818
[23] M. Irwanto. Solar Irradiance and Optimum Tilt Angle of Photovoltaic Module in Tanjung Morawa, North Sumatera, Indonesia. International Journal of Research in Advanced Engineering and Technology, 2015; 1(1):34-38.
[24] Kamrul Islam Chowdhury, Md.Iftekharul Alam, Promit Shams Bakshi. Performance Comparison between Fixed Panel, Single-axis and Dual-axis Sun Tracking Solar Panel System. Thesis in BRAC University, Bangladesh, 2018.
[25] Muhammad Bilal, Muhammad Naeem Arbab, Muhammad Zain Ul Abideen, Afridi, Alishpa Khattak. Increasing the Output Power and Efficiency of Solar Panel by Using Concentrator Photovoltaics (CPV).International Journal of Engineering Works.2016;3(12):98-102.